

## Chapter 10

### Imaging Exoplanets

#### *The Role of Small Telescopes*

B. R. Oppenheimer

*American Museum of Natural History, Department of Astrophysics  
Central Park West at 79<sup>th</sup> Street, New York, NY USA*

A. Sivaramakrishnan, R. B. Makidon

*Space Telescope Science Institute  
3700 San Martin Dr., Baltimore, MD USA .*

**Abstract:** The principal difficulties in directly imaging extremely faint objects in orbit about nearby stars stem not from the sensitivity or collecting area of telescopes, but rather from the fact that the central star's light drowns out the signal of the faint companion. We have conducted extensive simulations of very high-order adaptive optics (AO) systems with coronagraphic imagers on relatively small telescopes. High-order AO and optimized coronagraphs enable small ( $< 4\text{m}$ ) telescopes to play a critical role in the burgeoning effort to image exoplanets. The key to understanding the benefits of outfitting a 2 to 4m telescope with extremely high-order AO systems lies in the nature of the AO correction. An AO system with  $N_{\text{act}}$  actuators projected across the linear diameter,  $D$ , of the telescope's pupil can correct the point spread function (PSF) of a star on the optical axis within the angle  $\theta_{\text{AO}} = N_{\text{act}}^{-1}/2D$ . For a system with  $N_{\text{act}} = 10$ , the AO system corrects the PSF within  $5\theta_{\text{AO}}$ , or five times the diffraction limit. As  $N_{\text{act}}$  is increased, successively improved suppression of the seeing halo results, opening a large, as yet unexplored, part of the mass-separation parameter space relevant to faint companion science. For example, an optimized coronagraph behind a 941 element ( $N_{\text{act}} = 34$ ) AO system on a 3.6m telescope is capable of detecting objects  $>14$  magnitudes fainter than the central star at separations between 0.2 and 1.5 arcsec in the  $H$ -band. Such a system will also solve or quantify many of the problems that exoplanet imaging projects must face in the near future.

**Key words:** extrasolar, planet, adaptive optics, coronagraphy, brown dwarf, point spread functions

## 1. INTRODUCTION

In 1994 Angel published a startling set of calculations. He showed, convincingly, for the first time, that the direct imaging and even low-order spectroscopic study of planets orbiting stars other than the Sun (a.k.a. “exoplanets”) is not only possible using ground-based telescopes, but also feasible within a decade or two. If Angel’s (1994) calculations are shown to be correct, obtaining such images would represent the solution of perhaps one of the longest standing problems in modern astronomy. Indeed, Immanuel Kant (1755) devoted an entire section of his *Allgemeine Naturgeschichte und Theorie des Himmels* to what such planets might be like and who would inhabit them, based on Newtonian physics. In 1733 Alexander Pope, musing about “worlds unnumbered” wrote the following in “An Essay on Man” (a poem which, in its entirety, provides perhaps the best justification for all academic and basic research).

He, who through vast immensity can pierce,  
See worlds on worlds compose one universe,  
Observe how system into system runs,  
What other planets circle other suns,  
What varied Being peoples every star,  
May tell why Heaven has made us as we are.

Although the empirical methods of science could not until recently provide evidence for the existence of Pope’s “other planets,” they did not restrain Kant, nor many generations of future scientists, novelists and the interested public, from speculating. The idea of exoplanets is older than empiricism, but the scientific evidence for them is new, and the detailed study of their physics, chemistry and geology has not begun.

Shortly after Angel’s paper appeared, the indirect discovery of a body, roughly the mass of Jupiter orbiting a bright, visible star was announced (Mayor and Queloz 1995). The following week saw the publication of the first images and the Jupiter-like spectrum of a substellar companion of a nearby star (Nakajima et al. 1995; Oppenheimer et al. 1995). To date, over one hundred extrasolar planets and a handful of brown dwarf companions of other stars have been found through the radial velocity method, which detects the reflex motion of the star due to the gravitational influence of the orbiting body (Marcy and Butler 2000). Almost two-dozen spectra of free-floating, cool brown dwarfs have been obtained (e.g. Burgasser et al. 2001). With the benefit of this knowledge, the problem of direct imaging of exoplanets has been greatly refined. Herein we set out to specify the

problem anew and examine solutions, with particular attention to the already fruitful adaptive optics (AO) coronagraphy technique.

Telescopes smaller than 4-m in diameter with AO and coronagraphs play a crucial role in the ultimate goal of imaging exoplanets because they fulfil a necessary set of precursor experiments, not only to establish and test the needed technologies for larger scale space-based projects, but also to begin the systematic investigation of the physics of faint companions.

## 2. THE MASS-SEPARATION PARAMETER SPACE

The parameter space relevant to the search for objects orbiting nearby stars is defined by the mass of the object,  $M$ , and its orbital separation,  $a$ . This seems simple to comprehend, but the sensitivity of a direct observing campaign is not uniform in the physically fundamental  $M$ - $a$  parameter space, primarily because direct techniques are sensitive to the observed quantities brightness and angular separation. For stellar companions of stars within a given volume-limited sample, brightness can be converted into  $M$  and the distribution of distances in the sample determines the coverage in  $a$ . However, in detecting substellar companions, those below the hydrogen burning limit, the conversion between the companion's brightness and  $M$  is not straight-forward. Indeed, brown dwarfs and planets (the principal objects presumed to exist in the parameter space of interest) cool with time. The cooling introduces an additional parameter, the age. In a volume-limited sample of stars, the ages of the stars are not, in general, measurable.

In the case of the indirect searches the sensitivity to mass is uninfluenced by age, but the parameter space is also explored in a non-uniform manner because of the large phase space of potential orbits defined by orbital period, mass and eccentricity, and also because the timing of observations in these surveys is neither uniform nor complete. For example, a survey that observes monthly has no sensitivity to orbital periods that are an integer multiple of one month. (Unfortunately, this incompleteness and the corresponding corrections to the statistical interpretation of the existing radial velocity surveys has still not been properly assessed, although the technique has been explored by Nelson and Angel 1998.) Thus, the mass-separation parameter space for the entire sample of stars in radial velocity surveys is not uniformly sampled, although for individual stars, large parts of the  $M$ - $a$  plane may be well-explored.

Figure 1 displays the  $M$ - $a$  parameter space for substellar values of  $M$  and solar system scales for  $a$ . The regions that have been probed by the indirect and direct techniques to-date are also indicated. Figure 1 clearly shows that neither indirect nor direct techniques have covered even the majority of the

$M$ - $a$  parameter space in the regime of substellar objects ( $M < 0.08 M_{\odot}$ ) and solar system scales ( $a < 50$  AU). For example, an analog of Jupiter is barely detectable and a Saturn analog is completely inaccessible now. Furthermore, comparison between the direct and indirect observing methods is difficult because the overlap in parameter space is only now beginning to exist.

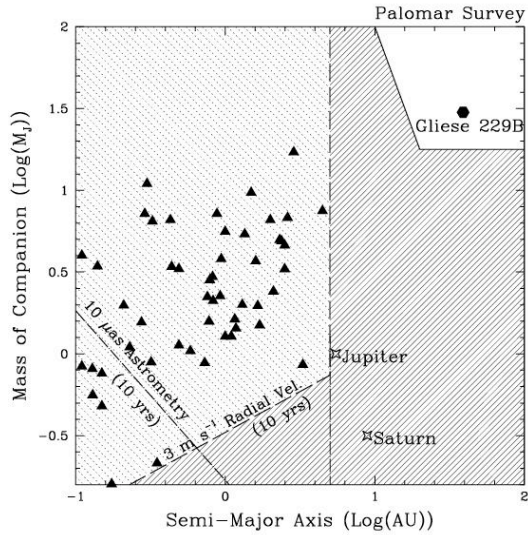


Figure 1. Mass,  $M$ , versus separation,  $a$ , for substellar companions and solar system scales, shown on a logarithmic scale in both axes. Mass is in units of the mass of Jupiter,  $M_J$ , and separation is in units of astronomical units (AU). The shaded regions indicate areas probed by surveys to date (see text). The region in the upper right corner, surveyed by Oppenheimer et al. (2001) using a 1.5-m telescope, is the only complete direct imaging survey to enter this parameter space. On the left, the lightly shaded region has been non-uniformly probed by the  $3 \text{ m s}^{-1}$  radial velocity searches. The dash-dot line indicates the region accessible to an indirect astrometric search lasting 10 years. To date, no survey of any kind has probed the darkly shaded region, although a few observations of individual stars have probed parts of it.

Although the regions of the  $M$ - $a$  plane surveyed by the indirect techniques have not been uniformly sampled, tremendous progress has been made (e.g. Marcy and Butler 2000 and references therein). Within the next decade serious treatment of the general physics of companions around G, K and F main sequence stars will be possible with the results from the indirect surveys alone. Ideally, a complete study of this parameter space should cover all relevant ranges of  $M$  and  $a$ , for all types of primary stars. Furthermore, the true nature of the companions themselves can only be determined through spectroscopic measurements. For these reasons, the techniques must be improved such that they can reach ranges in  $M$  and  $a$  comparable to those of the indirect techniques. This can be achieved with high-order AO and coronagraphy on ground-based telescopes. Other authors

have made similar suggestions in the past. (See for example, Angel 1994 or Sandler and Angel 1997). However, what has not hitherto been widely appreciated is that a large part of the  $M$ - $a$  parameter space is accessible to AO coronagraphs on telescopes smaller than 4-m.

The first consideration in support of this assertion is summarized in Table 1, which shows the required angular resolution of the imaging system used. Considering only the spatial resolution needed, a 4-m telescope operating at the diffraction limit at a wavelength,  $\lambda = 1 \mu\text{m}$  (achievable with AO already), would be capable of resolving physical distances as small as 1 AU around some 2000 stars known within 20 pc. This wavelength is chosen because both observations of brown dwarfs and models of exoplanets show that these cool objects peak in their spectral energy distributions near  $1 \mu\text{m}$  (e.g. Oppenheimer et al. 2000b).

Table 1.  
Telescope Diffraction Limit Requirements For Direct Imaging Surveys

Distance	5 pc	10 pc	15 pc	30 pc
Max. Ang. Separation: 1 AU orbit	200 mas	100 mas	67 mas	33.3 mas
Required Telescope Diameter for observations at $\lambda = 1 \mu\text{m}$	1.05-m	2.1-m	3.1-m	6.2-m
$J$ -band Limiting Mag. (5 $\times$ 1000s)	19.5	21	21.8	23.4
Approx. No. Stars Known	64	325	877	3508

Telescope diameter is determined by the angular resolution required for 1 AU physical resolution at the given distance. The  $J$ -band limiting mag. is an approximation for field point-source detection based on existing state-of-the-art instruments without AO for the telescope aperture given.

However, challengingly small angular separation is not the only difficulty facing a would-be planet hunter. Let us also briefly examine the predicted brightness of a Jupiter sized companion. By reflected light, Jupiter at 5 AU from the Sun viewed from outside the solar system is approximately 18 magnitudes fainter than the Sun (Woolf and Angel 1998). For the purposes of argument, let us assume that a clever optical technique can completely remove the starlight from an exoplanetary system, so that the only object left in our hypothetical image is that of the Jupiter analog. The brightness of the exo-Jupiter is determined solely by the brightness of the parent star. Table 1 shows that a 3m telescope is capable of detecting point sources without adaptive optics that are as faint as 22 mag. in  $J$ -band. Thus, stars brighter than  $J = 4$  could be searched with reasonable exposure times for gas giant planets.

These arguments serve to show simply that the telescope aperture is not, *a priori*, the limiting factor in the direct imaging of exoplanets. Indeed, the principal problem is finding that “clever optical technique” mentioned above that can remove all or most of the central star’s light. The most important

element limiting the direct detection of planets is the point spread function (PSF) of the telescope optics and the atmosphere. The light of the primary star, in practical situations, is predominantly outside of the diffraction limited Airy pattern. Indeed, typical “seeing” results in images on the order of 5 to 80 times wider than the angular separations listed in Table 1, with residual light levels extending many arcseconds away from the star centroid. (See, for example King 1971 or Racine 1996). Adaptive optics can control the seeing and coronagraphy can reduce the amount of remaining light from the central star. To understand the utility and efficacy of these techniques, we must first understand the various components of the PSF, particularly with an adaptive optics system in operation. As a figure of merit in the following discussion, we rely heavily upon the Strehl ratio, defined as the ratio of the peak intensity of an actual PSF to that of an ideal, perfect, diffraction-limited PSF.

### 3. LIGHT: THE FUNDAMENTAL LIMIT

In any signal processing problem, the detection of a signal is dependent on the noise present. In the case we explore here, the signal is light from an exosolar system and the processor is the telescope, AO system, science camera and software. At the location of a faint planet on the science detector, there are several sources of noise, including detector read noise, sky background and any other source of contaminating light. When a bright star is present, even for the shortest duration exposures, the light of the star is, by far, the dominant source of noise impeding the detection of the planet. In order to detect that planet, the random fluctuations in the wings of the star’s PSF at the location of the planet must be *at least* a few times smaller than the signal from the planet. One proposed plan of attack on this problem is to marginally reduce the starlight with AO and then simply increase the telescope aperture  $D$  to the point where integrations yielding  $\sqrt{N_{\text{planet}}}/\sqrt{N_{\text{star}}} > 3$  are practical. (Here  $N_{\text{planet}}$  is the number of photons detected from the planet and  $N_{\text{star}}$  is the number of photons from the star that are superimposed on the location of the planet.) In fact, it is more efficient, at this point in time, to devote astronomical resources to the reduction of  $N_{\text{star}}$ . Indeed, this is a cheaper, possibly faster route to a cleaner, less contaminated portrait of an exosolar system. Note that as  $D$  increases, telescope cost increases approximately as  $D^2$  to  $D^4$  (Schmidt-Kaler 1997), and the necessary AO system complexity and cost also rise as  $D^2$ .

Let us examine the PSF assuming that the telescope optics are diffraction limited (e.g.  $\lambda/10$  at  $0.65 \mu\text{m}$ ) and free of ghost reflections or light sources exterior to the field of view. In this case, the PSF is dominated by structure

due to turbulence in the atmosphere. Microfluctuations in the air temperature throughout the atmosphere above an observatory translate into microfluctuations in the air's index of refraction. These result in the random disruption of the phase of the planar wave front of light from the distant star. The turbulence is blown past the telescope aperture by winds with speeds on the order of  $10\text{-m s}^{-1}$ . Substantial work on the structure and theory of this turbulence has provided useful guidelines on how to correct it, and the body of knowledge and the set of AO instruments that do correct it, at least partially, is growing rapidly. We do not intend to review this material here. Instead, the goal is to provide an understanding of the next few steps necessary for the nearly perfect AO correction that permits planet detection, or at least access to the unprobed regions of the  $M$ - $a$  parameter space.

### 3.1 How to Reach 95% Strehl Ratios

In a real, operating AO system, the PSF after correction is characterized by a sharp, diffraction limited core, sometimes with bright rings visible, along with a broad “seeing halo” which corresponds in width and shape to the uncorrected image. Typical Strehl ratios achieved are near .4 to .7. It is important to appreciate that the sensitivity to faint companions is an extremely strong function of the Strehl ratio. (See also Section 4). Once the Strehl ratio exceeds 90%, faint companion detection efficiency improves hyperbolically, such that an improvement from 96 to 97% results in almost an order of magnitude increase in sensitivity. There are a number of effects that prevent existing AO systems from producing PSFs with Strehl ratios above 70%:

- Wave front fitting error, due to finite spatial sampling of the wave front and a finite number of correcting elements whose arrangement does not span all scales of turbulence
- The time-lag error based on the control loop's update frequency and the wind speed during observations
- Wave front sensing error due to a finite number of photons available from the guide star
- Residual alignment error and PSF calibration, i.e. it is difficult to establish the set of control parameters used to drive the control loop to produce a perfect PSF

The fourth issue itemized above can be solved without any major innovation in technology. Residual alignment error can be addressed through additional, lower bandwidth control loops that actively maintain precise alignment throughout the system without incurring extreme costs. PSF calibration, a stumbling block for many existing AO systems, is ultimately a solvable problem using bright calibration sources that permit

software, such as phase diversity solutions, to detect extremely low-level aberrations in the final AO system PSF. This is done without the need for telescope time allocated at night.

The first two items in the list above can be addressed essentially by increasing the number of correcting elements in the AO system and speeding up the duty cycle. However this cannot be done arbitrarily. Item 3 constrains the total number of actuators and the update frequency. Table 2 shows a calculation of the reduction of Strehl ratio as a function of the number of actuators placed in a grid on a 3.6-m telescope, with a 4<sup>th</sup> magnitude star used as a guide star. The system efficiency is assumed to be 20%.  $N_{\text{act}}$  is the linear number of actuators placed across the telescope pupil, while  $N_{\text{tot}}$  is the total number of actuators filling the pupil. The update frequency is assumed to be 5 kHz. Clearly, increasing  $N_{\text{act}}$  beyond 64 results in Strehl degradations that are disadvantageous. The numbers in Table 2, which should be treated as theoretical limits given the system throughput, can only be improved with superior wave front sensing technology. They serve as a useful benchmark for this discussion.

Table 2.

Degradation of Strehl ratio due to number of photons available in each subaperture. The guide star is 4th magnitude, update frequency is 5 kHz, efficiency is 20%, telescope aperture is 3.6m.

$N_{\text{act}}$	4	8	16	34	64	128
$N_{\text{tot}}$	12	50	201	907	3216	12867
Strehl “hit” at 0.8 $\lambda$ m	0.0 %	0.0%	0.1%	0.4%	1.5%	6.0%
Strehl “hit” at 1.6 $\lambda$ m	0.0 %	0.0%	0.0%	0.1%	0.4%	1.5%

Addressing the issues in this section with a high order AO system can bring the PSF to a Strehl ratio near 95%. We demonstrate this claim in the following section detailing our simulations that include all of the effects itemized above. Then, in Section 3.4, we describe further problems and improvements needed to achieve Strehl ratios above 95%, the regime where coronagraphy and nulling provide the largest gains in tandem with AO.

### 3.2 Image Improvement by AO

AO PSF improvement is manifest only within a maximum radial distance,  $\lambda_{\text{AO}}$ , from the center of the PSF (Sivaramakrishnan et al. 2001). This distance is determined by the linear actuator density, the telescope aperture,  $D$ , and the observing wavelength,  $\lambda$ . To understand this intuitively, one can think of AO correction as a high pass filter acting on spatial phase variations of incoming wave fronts. The AO system's spatial frequency

cutoff is  $k_{AO} = N_{act}/2D$ , where  $N_{act}$  is the number of deformable mirror actuators projected across the telescope's primary mirror. Since the electric field at the image plane is the Fourier transform of the field in the pupil plane,  $k_{AO}$  translates to an angle  $\Delta_{AO} = N_{act}\lambda/2D$  on the sky. Thus AO only improves the point spread function within a radius  $\Delta_{AO}$ .

Furthermore, even a perfectly corrected image from an AO system has bright rings because the point spread function is the diffraction pattern generated by the telescope's aperture. These bright rings swamp all faint structure around a central on-axis source. (For clarity, the Airy pattern is specific to an unobscured circular pupil and is not, in general, the shape of a telescope's PSF.)

### 3.3 Halo Suppression from High-Order AO

For low-order AO systems ( $N_{act} \sim 10$ ),  $\Delta_{AO}$  is close to the angular size of the third or fourth ring ( $\sim 5 \lambda / D$ ) of the perfect, diffraction-limited PSF. As a result, a diffraction limited core is seen in the corrected images, but the bright “seeing halo” remains mostly unaffected.

High-order AO (where  $N_{act} > 10$  or  $\Delta_{AO} > 5 \lambda / D$ ) suppresses the seeing halo, which permits an increased dynamic range in the final image. The amount of suppression can be quantified with the following simplistic expression.

$$\Delta = \frac{S_{AO}}{S_{see}} (1 - S_{AO})^{\Delta}$$

Here,  $\Delta$  is the contrast enhancement provided by the AO correction.  $S_{AO}$  and  $S_{see}$  are the Strehl ratios of the AO-corrected image and the image made through natural seeing conditions, respectively. The first factor in this expression is the contrast improvement due to sharper images (i.e. the increase in the peaks of the point source images). The second factor represents the contrast improvement due to the removal of light from the seeing halo. In other words, not only is the faint object's PSF more sharply peaked, but the background of light from the central star is reduced. Both effects lead to detection gains.

For existing AO systems such as those at Palomar and Lick,  $\Delta$  is approximately 30 to 40. Figure 2 compares the expected PSFs of a 3.6-m telescope with  $N_{act} = 12$  and 34, at an observing wavelength of  $\lambda = 1.6 \mu\text{m}$ . The importance of the increased number of actuators is apparent. For  $N_{act} = 34$ , the PSF has a profoundly darker region within 1.5 arcsec as compared to the lower-order AO system. In this case,  $\Delta$  is approximately 500. For  $N_{act} = 12$ , close in performance to the Palomar AO system,  $\Delta$  is about 45. This is a

direct consequence of correcting the higher frequency components of the wave front. This clearly shows that increasing  $N_{\text{act}}$  provides tremendous gains in the search for faint objects in orbit about nearby stars. (Details of the simulation techniques are described in Sivaramakrishnan et al. 2001.)

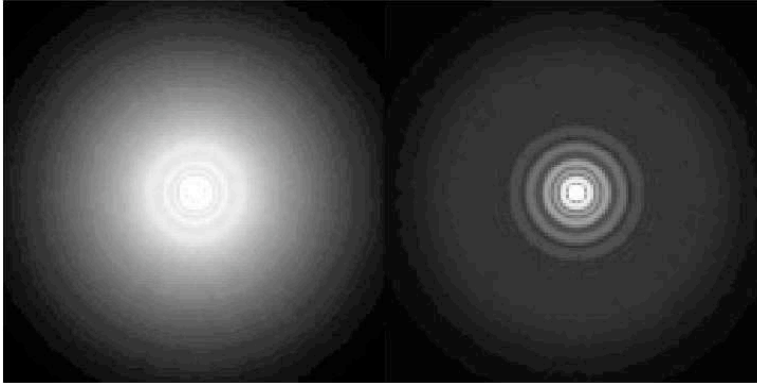


Figure 2. AO PSF simulations for  $N_{\text{act}} = 12$  (left) and 34 (right) in  $H$ -band using 1000 independent atmospheric phase screen realizations with cell size one 15<sup>th</sup> of the telescope diameter (3.6-m). Phase screens are scaled to 40 wavelengths across the  $H$ -band and passed through a simulated AO system to demonstrate broad-band performance. The effect of increasing  $N_{\text{act}}$  is manifest in the suppression of the halo in the right hand image within the radius 1.5 arcsec. (See Sivaramakrishnan et al. 2001 for further details.) The Strehl ratios are 0.69 and 0.89 for the left and right PSFs respectively.

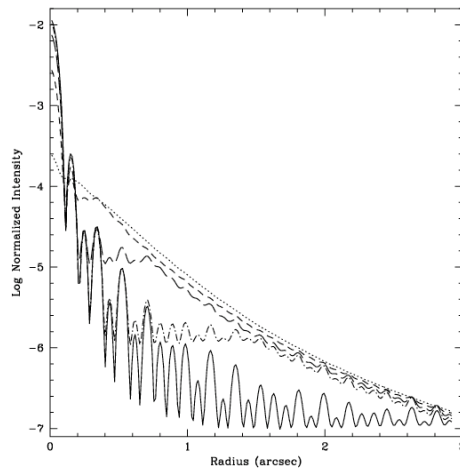


Figure 3. Radial profiles of simulated AO PSFs for a 3.6-m telescope with  $N_{\text{act}} = 4, 8, 16, 34$  and 64 (from top to bottom at the 1 arcsecond radius) with median Mauna Kea seeing in  $H$ -band (1.6  $\mu\text{m}$ ). The Strehl ratios are 0.05, 0.23, 0.63, 0.87 and 0.96 respectively. Note the superior halo clearing as  $N_{\text{act}}$  increases.  $\lambda_{\text{AO}}$  is the radius of the “shoulder” in the PSF.

These simulations include all of the effects described in Section 3.1. Figure 3 shows radial profiles of similarly simulated PSFs on a 3.6m telescope subjected to median seeing conditions at a good site, such as Mauna Kea. Radial profiles are shown for each of the values of  $N_{\text{act}}$  used in Table 2. Beyond  $N_{\text{act}} = 64$ , the simulations become unphysical because they do not include additional effects which we describe below.

### 3.4 Going Beyond 95% Strehl Ratio

Once the effects described in Section 3.1 are accounted for by a sufficiently high order, high speed AO system ( $N_{\text{act}} = 64$  at 5 kHz for a 3.6m telescope in Hawaii), Strehl ratios around 95% can be achieved at the 1 $\mu$ m wavelength of interest for faint companion studies. However, further improvements cannot be made simply by throwing a larger number of faster actuators at the problem. Indeed, we showed above that for more than 64 actuators across the pupil, there are not enough photons available to permit accurate AO correction (Table 2). Furthermore, additional natural and instrumental effects become important when Strehl ratios above 95% are needed. These effects include speckle noise, atmospheric scintillation, differential refraction and dust or microroughness in the optics.

Speckle noise is an effect that amplifies the noise level in the halo beyond the simple expression  $\sqrt{\epsilon_{\text{star}}}$ . Speckle noise is due to the persistence of remnant speckles in an AO image. Bright spots approximately the size of the diffraction limit wander about. In long exposures these average into the seeing halo, but the accumulation of photons in any given pixel is not governed by simple Poisson statistics because of the behavior of these speckles. A number of investigators have researched the effects of speckle noise. Pessimistic views (Sandler and Angel 1997, Racine 1999) suggest that the effect requires image integration times that must be modified by a factor related to the effective speckle lifetime (which is on the order of milliseconds). Other studies show that the spatial distribution of speckles is actually strongly correlated with the structure of the PSF, such that the speckles tend to exist in bright parts of the PSF (such as the bright rings surrounding the core) far more frequently than elsewhere (Bloemhof et al. 2001). Sivaramakrishnan et al. (2002) show that such “first order” speckle patterns necessarily form a perturbation (to the perfectly corrected PSF) which is antisymmetric about its center. In any case the principal effect is that integration times must be somewhat longer than those expected from Poisson statistics. This is not particularly prohibitive, and speckle noise loses its significance when a coronagraph or nulling technique is used because the speckles themselves are also suppressed.

Atmospheric scintillation is a low level effect investigated most thoroughly by Dravins (1997a, 1997b, 1998). The atmosphere's turbulence affects not only the phase but also the amplitude of the star's wave front at a level of about 1 part in  $10^6$ . Scintillation reduces the Strehl ratio by about 3 to 4% (e.g. Angel 1994) at a relatively good observing site. In principle scintillation can be corrected by an additional adaptive element and a second wave front sensor. This has not been investigated seriously yet, but it must be in the near future, when AO systems approach the 90 to 95% Strehl ratio regime.

Differential refraction is an effect that probably becomes important at Strehl ratios above 97 or 98% and is due to a very weak wavelength dependence of the index of refraction of air. Thus, in an AO system where the optical path difference is corrected without regard for wavelength dependence, image degradation will occur when broadband filters are used. Differential refraction probably affects the PSF at the level of one part in about  $10^7$  or  $10^8$ , although it has also not been properly investigated. (See Nakajima 1994). This effect is also not included in our simulations.

Furthermore, dust in the optical system or microscopic scratches and pits in the optics can scatter light over the entire field of view. Fortunately these effects result in a very low surface brightness, essentially uniform background. However, proper understanding of these effects is also needed since they represent an additional source of noise.

Finally, a few authors have raised the possibility that natural Zodiacal light in an exosolar system may prevent exoplanet imaging (e.g. Woolf and Angel 1998, Backman et al. 1998). However, this, too, is largely an unknown aspect of the problem. The amount of Zodiacal dust in our own system is not well quantified and comprehensive surveys of such optical dust disks around other stars are only possible with the techniques described in this paper.

Each of these effects absolutely must be assessed theoretically and measured observationally if very high Strehl ratios are ever going to be seen, especially from the ground. The precise contribution of these effects is unknown, but present indications are that they must be understood and controlled for imaging planets smaller than Jupiter around nearby stars. To this end, we discuss the use of a coronagraph behind the sort of high order AO system described above, capable of a 95% Strehl ratio in the near infrared wavelengths. Such a system, which would push current AO technology to its limit (as described in Section 3.1 to 3.3), will determine exactly how to go about solving the problems raised in this section.

#### 4. CONTRAST ENHANCEMENT BY CORONAGRAPHY

To demonstrate that much can be achieved immediately with systems approaching 90 to 95% Strehl ratios, we have simulated coronagraphic PSFs for  $N_{\text{act}} = 12$  and 34 on a 3.6-m telescope observing in the  $H$ -band (Sivaramakrishnan et al. 2001). These images, shown in Figure 4, directly complement those in Figure 2. The  $N_{\text{act}} = 34$  case shows that halo suppression and optimized coronagraphy reduce the starlight in the 0.2 to 1.5 arcsec range by a factor of more than 30, compared to the  $N_{\text{act}} = 12$  case. These simulations include all of the effects discussed in Section 3 except for those in Section 3.4.

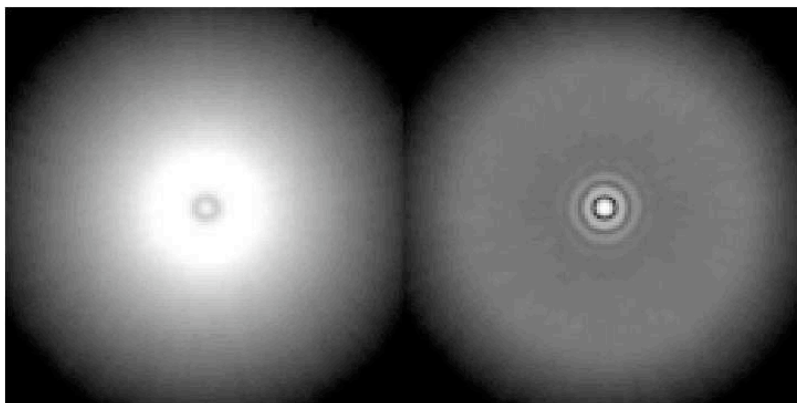


Figure 4. Simulated PSFs similar to those in Figure 2, but with coronagraphic optics inserted.

Using these simulations we can compute the faintest companion detectable in a long exposure image taken with such a system (accounting for detector characteristics, optical quality, positioning and manufacturing errors of 100 nm and thermal background). We compute this by considering the dynamic range, which we define as the difference in magnitudes between the central star and the faintest detectable point source at a given radius from the star. Figure 5 shows the dynamic range of a 3.6-m telescope fitted with an AO system with  $N_{\text{act}} = 34$  and an optimized coronagraph with active optics alignment and an additional high-speed tip-tilt system for image stability. Such a system is sensitive, in only 1000s, to companions more than 14 magnitudes fainter than the primary star.

One can construct a hypothetical survey with such an instrument imaging 300 nearby stars. Using the average ages of these stars as well as their distribution in distance from Earth and their magnitudes, we can compute the approximate region of the  $M$ - $a$  parameter space that such a survey would

probe. Figure 6 shows this region, which represents an almost 100 fold increase in the parameter space accessible to direct imaging techniques. We should be careful to remark that we have been conservative here, by only conducting these calculations for the  $N_{\text{act}} = 34$  case. The most important conclusion, however, is that a 3.6-m telescope outfitted with a high order AO system and an optimized coronagraph will, without doubt, permit the synergism of the indirect and direct techniques for faint companion detection, explore a virtually untouched region of the  $M$ - $a$  parameter space, and provide extremely important quantitative and empirical direction to the next few steps toward imaging exoplanetary systems.

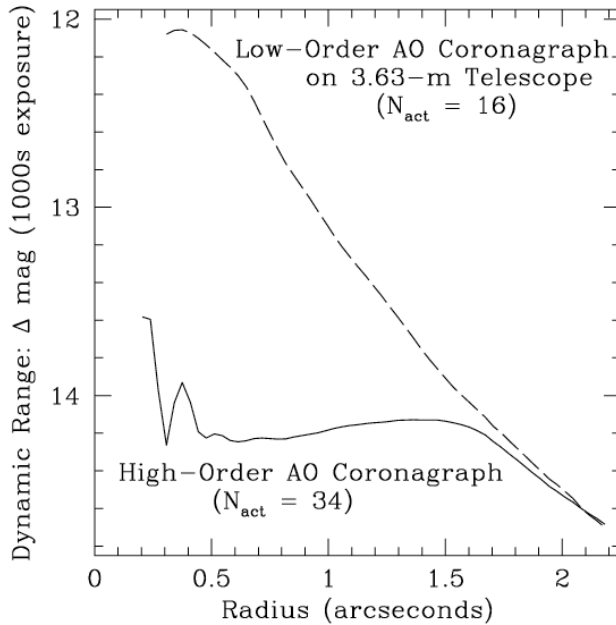


Figure 5. Dynamic range for coronagraphs behind AO systems with  $N_{\text{act}} = 12$  ("low-order") and  $N_{\text{act}} = 34$  ("high-order"). We have evaluated the accuracy of the simulations by comparing them directly with real Palomar AO Coronagraph observations (Sivaramakrishnan et al. 2001, Oppenheimer et al. 2000a).

Furthermore, a number of other techniques might be exploited to improve on Figure 6. Recent papers have suggested that the PSF can be "engineered" in order to provide regions that are particularly dark, i.e. small holes in the PSF where one could search for even fainter companions (e.g. Malbet et al. 1995). A system such as the one discussed here would be capable of testing such techniques and exploiting them for the first time.

Sivaramakrishnan et al. (2001) demonstrate that Lyot coronagraphs (Lyot 1939) are most effective with occulting spots that are at least  $4\lambda/D$  in diameter and when Strehl ratios are 80% or higher (except in the case of solar Lyot coronagraphs). (See Sivaramakrishnan et al. 2001 for a detailed description of the principles of Lyot coronagraphy.) When the Strehl ratio exceeds 95%, phase mask coronagraphs (Roddier and Roddier 1997, Rouan et al. 2000, Riaud et al. 2001) enable image core suppression and may be superior to Lyot coronagraphs.

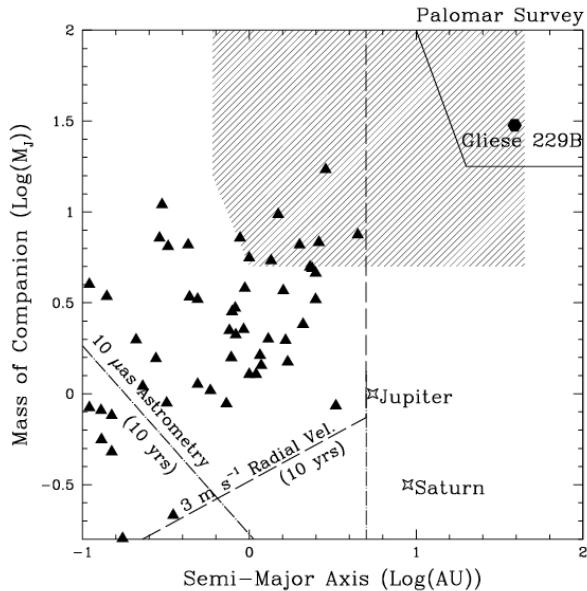


Figure 6. Same as Figure 1, but the shaded region indicates the parameter space accessible to the AO coronagraph and survey described in Section 4.

## 5. SEVEN REASONS TO PURSUE HIGH-ORDER AO ON 3 TO 4-m TELESCOPES

In conclusion and summary, there is substantial evidence that small telescopes can and will play a vital role in the mounting effort to image exoplanets. We have shown that the scientific gains to be gleaned from a high-order AO system with a coronagraph on a 3.6-m telescope are tremendous and will help solve many of the issues that this effort will face in the next two decades. We list of seven principal reasons why a small

aperture telescope should be fitted with a high order AO system and an optimized, diffraction-limited coronagraph:

- AO PSF calibration to extremely high precision will be solved.
- The true extent and importance of speckle noise, atmospheric scintillation and differential refraction will be measured.
- Innovative coronagraphic or nulling techniques will be evaluated, tested and refined.
- “PSF engineering” will be attempted for the first time on an astronomical telescope.
- Experience with extremely high-order AO will be acquired and some of the control issues surrounding these complex systems will necessarily be used to build the 30 to 100-m telescopes currently on the drawing board.
- A survey of Zodiacal light around other main sequence stars will be undertaken, determining whether this is an important concern for the exoplanet effort and probing the physics of exo-Zodiacal dust disks.
- A 100 fold increase in the  $M$ - $a$  parameter space accessible to direct imaging will result in the direct imaging of brown dwarfs and hot, super-Jupiter planets around stars within 30 pc. These objects will be prime targets of opportunity for coronagraphic spectrographs on larger telescopes.

## 6. REFERENCES

- Angel, J. R. P. 1994, “Groundbased imaging of extrasolar planets using adaptive optics,” *Nature*, **368**, 203
- Backman, D.E., Caroff, L.J., Sandford, S.A., and Wooden, D.H. 1998, “Exozodiacal Dust Workshop, Conference Proceedings,” NASA/CP-1998-10155.
- Bloemhof, E. E., Troy, M., Dekany, R. G., Oppenheimer, B. R. 2001, “Behavior of remnant speckles in an adaptively corrected imaging system,” *Astrophys. J. Lett.*, **558**, L71
- Burgasser, A. J., Kirkpatrick, J. D., Brown, M. E., Reid, I. N., Burrows, A., Liebert, J., Matthews, K., Gizis, J. E., Dahn, C. C., Monet, D. G., Cutri, R. M., Skrutskie, M. F. 2001, “The Spectra of T Dwarfs I: Near-Infrared Data and Spectral Classification,” *Astrophys. J.*, **563**, in press
- Dravins, D., Lindegren, L., Mezey, E., Young, A. T. 1997a, “Atmospheric Intensity Scintillation of Stars. I. Statistical Distributions and Temporal Properties,” *Pub. Astron. Soc. Pac.*, **109**, 173
- Dravins, D., Lindegren, L., Mezey, E., Young, A. T. 1997b, “Atmospheric Intensity Scintillation of Stars. II. Dependence on Wavelength,” *Pub. Astron. Soc. Pac.*, **109**, 725
- Dravins, D., Lindegren, L., Mezey, E., Young, A. T. 1998, “Atmospheric Intensity Scintillation of Stars. III. Effects for Different Telescope Apertures,” *Pub. Astron. Soc. Pac.*, **110**, 610
- Kant, I. 1755 in *Allgemeine Naturgeschichte und Theorie des Himmels*, Section 3, public domain, English translation by I. Johnston: <http://www.mala.bc.ca/~johnstoi/kant1.htm>

- King, I. R. 1971, "The Profile of a Star Image," *Pub. Astron. Soc. Pac.*, **83**, 199
- Lyot, M. B. 1939, "Study of the solar corona and prominences without eclipses," *Mon. Not. Royal Astron. Soc.*, **99**, 578
- Malbet, F., Liu, D. T., Yu, J. W., Shao, M. 1995, "Space Adaptive Optics Coronagraphy," in *Space Telescopes and Instruments*, P. Y. Bely; J. B. Breckinridge, eds., Proceedings of SPIE, Vol. 2478, 230
- Marcy, G. W., and Butler, R. P. 2000, "Planets Orbiting Other Suns," *Pub. Astron. Soc. Pac.*, **112**, 137
- Mayor, M., and Queloz, D. 1995, "A Jupiter-Mass Companion to a Solar-Type Star," *Nature*, **378**, 355
- Nakajima, T. 1994, "Planet detectability by an adaptive optics stellar coronagraph," *Astrophys. J.*, **425**, 348
- Nakajima, T., Oppenheimer, B. R., Kulkarni, S. R., Golimowski, D. A., Matthews, K., and Durrance, S. T. 1995, "Discovery of a Cool Brown Dwarf," *Nature*, **378**, 463
- Nelson, A. F. and Angel, J. R. P. 1998, "The Range of Masses and Periods Explored by Radial Velocity Searches for Planetary Companions," *Astrophys. J.*, **500**, 490
- Oppenheimer, B. R., Kulkarni, S. R., Matthews, K., Nakajima, T. 1995, "Near IR spectrum of the cool brown dwarf GL 229B," *Science*, **270**, 1478
- Oppenheimer, B. R., Dekany, R. G., Hayward, T. L., Brandl, B., Troy, M., and Bloemhof, E. E. 2000a, "Companion detection limits with adaptive optics coronagraphy" in *Adaptive Optical Systems Technology*, P. L. Wizinowich, ed., Proceedings of SPIE, Vol. 4007, 899
- Oppenheimer, B. R., Kulkarni, S. R. and Stauffer, J. R. 2000b in *Protostars and Planets IV*, V. Mannings, A. Boss and S. Russell, eds. (Tucson: University of Arizona Press)
- Oppenheimer, B., R., Golimowski, D. A., Kulkarni, S. R., Matthews, K., Nakajima, T. 2001, "Coronagraphic Survey for Companions of Stars within 8 Parsecs," *Astron. J.*, **121**, 2189
- Pope, A. 1733, *An Essay on Man*, public domain
- Racine, R. 1996, "The Telescopic Point-Spread Function," *Pub. Astron. Soc. Pac.*, **108**, 699
- Racine, R., Walker, G. A. H., Nadeau, D., Doyon, R., and Marois, C. 1999, "Speckle Noise and the Detection of Faint Companions," *Pub. Astron. Soc. Pac.*, **111**, 587
- Riaud, P., Boccaletti, A., Rouan, D., Lemaquis, F., Labeyrie, A. 2001, "The Four-Quadrant Phase Mask Coronagraph. II. Simulations," *Pub. Astron. Soc. Pac.*, in press.
- Roddier, F., and Roddier, C. 1997, "Stellar Coronagraph with Phase Mask," *Pub. Astron. Soc. Pac.*, **109**, 815
- Rouan, D., Riaud, P., Boccaletti, A., Clénet, Y., and Labeyrie, A. 2000, "The Four-Quadrant Phase-Mask Coronagraph. I. Principle," *Pub. Astron. Soc. Pac.*, **112**, 1479
- Sandler, D. G., and Angel, J. R. 1997, "Direct imaging of extra-solar planets from the ground using adaptive optics," in *Optical Telescopes of Today and Tomorrow*, Arne L. Ardeberg, ed., Proceedings of SPIE, Vol. 2871, 842
- Schmidt-Kaler, T. 1997, "Telescope costs and cost reduction," in *Optical Telescopes of Today and Tomorrow*, A. L. Ardeberg, ed. Proceedings of SPIE Vol. 2871, 635
- Sivaramakrishnan, A., Koresko, C. D., Makidon, R. B., Berkefeld, T., and Kuchner, M. J. 2001, "Coronagraphy with High-Order Adaptive Optics," *Astrophys. J.*, **552**, 397
- Sivaramakrishnan, A., Lloyd, J. P., Hodge, P. R. and Macintosh, B. E. 2002, "Speckle Decorrelation and Dynamic Range in Speckle Noise-limited Imaging," *Astrophys. J., Lett.*, **581**, L59
- Woolf, N. and Angel, J. R. P., 1998, "Astronomical Searches for Earth-Like Planets and Signs of Life," *Ann. Rev. Astron. Astrophys.*, **36**, 507